A MIXED SIDESLIP YAW RATE STABILITY CONTROLLER FOR OVER-ACTUATED VEHICLES

Alex Gimondi[1], **Matteo Corno**[1], **Sergio M. Savaresi**[1]

[1] Dipartimento di Elettronica, Informazione e Bioingegneria, Politecnico di Milano, Piazza Leonardo da Vinci 32, 20133 Milan, Italy

ABSTRACT

Electronic stability control (ESC) has become a fundamental safety feature for passenger cars. Commonly employed ESCs are based on differential braking. Nevertheless, electric vehicles' growth, particularly those featuring an over-actuated configuration with independent wheel motors, allows for maintaining driveability without slowing down the vehicle. Standard control strategies are based on yaw rate tracking. The reference signal is model-based and needs precise knowledge of the friction coefficient. To increase the system robustness, more sophisticated approaches that include vehicle sideslip are introduced. Still, it is unclear how the two signals have to be weighted, and rarely proposed controllers have been experimentally validated. In this paper, we present a mixed sideslip and yaw rate stability controller. The mixed approach allows to address the control design as a single-input single-output problem simplifying the tuning process. Furthermore, we explain the rationale behind the choice of the weighting parameter. Eventually, the proposed ESC is validated following EU regulation in simulation and with an experimental vehicle on dry asphalt and snow. The results obtained in all the performed tests demonstrate that the proposed control strategy is robust and effective. The mixed approach is able to halve the sideslip in critical conditions with respect to a pure yaw rate approach.

1 INTRODUCTION

Electronic stability control (ESC) maintains car driveability in critical situations avoiding the car from spinning or drifting [1]. It is also known as vehicle stability control (VSC) or direct yaw control (DYC). The most famous system, the Bosch ESP [2], proved to reduce casualties significantly [3]. Common ESCs are based on differential braking, *i.e.* they generate a yaw moment by independently braking each wheel; this inevitably causes the vehicle to slow down.

Nowadays, full electric vehicles (FEV) attract more and more attention thanks to their ecological potential. Between different electrical power train configurations, particular interest has to be devoted to the one with four-wheel drive (4WD). This feature can be achieved both with in-wheel or chassis-mounted electric motors. In any case, the advantages of electric motors, *e.g.*, precise torque modulation, fast response, added to the possibility of independently drive each wheel open new opportunities for vehicle dynamics control [4, 5].

The general problem of controlling the vehicle yaw motion can be faced in different ways. We restrict our analysis to the systems featuring a similar actuator architecture, thus avoiding considering active steering. DYC approaches can be divided into three philosophies [6]: yaw rate control, sideslip control, and combined control. Concerning the first one, [7] presents a robust control approach, however it is not validated in challenging situations. A good comparison of control techniques can be found in [8] in which eventually a PID is chosen. In [9], a second-order sliding mode control have been used in simulation, [10] implemented an integral sliding mode controller on a test vehicle. In [11], a linear quadratic regulator (LQR) is implemented to track a reference yaw rate. On the other side, sideslip approaches are used to control the vehicle at the limit of handling since it is strictly related to vehicle instability and the capability of exerting yaw moment [12].

Regarding the combined control, three types of strategies can be found. Yaw rate and sideslip can be both controlled, e.g., [13–15] propose a sliding mode control, while [16, 17] use a LQR strategy. No one of these articles validate the proposed control using an experimental setup. Although the quality of high fidelity simulators on which the algorithms have been tested, often they do not accurately represent all the involved dynamics. Furthermore, as stated in [18]: "it is not possible to control the yaw rate and the sideslip angle independently, using only the yaw moment Mz. Trying to control both properties leads to a function-

ally uncontrollable system with uncontrollable directions. Controlling the lateral velocity (or the sideslip angle) and the yaw rate is possible only by including an additional device like an active steering system." Thus, a preference between yaw rate and sideslip tracking has always to be introduced, but seldom it is discussed. The second approach proposes to switch from yaw rate to sideslip control when critical conditions are reached, an example can be found in [8]. Nevertheless, derive the stability of a switching system and manage the switching phase is not trivial at all [19]. The third approach suggests to modify the reference signal, to the best of author's knowledge, this methodology is proposed only in [20], in which the reference signal is diminished to keep the sideslip below a certain threshold.

Eventually, after literature analysis the authors highlight the fact that: the majority of the contributions have been validated in simulation only, it is not suggested to control independently both yaw rate and sideslip, there is only one contribution that uses a similar approach, but it constrains the sideslip angle and has parameters to be adapted according to the desired performance.

Therefore, in this paper, we propose an ESC for a 4WD FEV capable of stabilizing the vehicle in severe conditions. In particular, we describe a mixed strategy that merges yaw rate and sideslip to cast the single-input multiple-output system in a single-input single-output (SISO) one. In addition, the choice of the mixing parameter is motivated. The stability control features a reference generation robust with respect to friction variations. The proposed solution has been validated in simulation (following ISO standards) and with an experimental vehicle; in this case vehicle sideslip has been estimated using [21]. The mixed approach greatly increases vehicle stability by halving the sideslip peak in critical situations.

The article is organized as follows. Section 2 presents the main models used for control design. Section 3 explains the ESC architecture analysing each block, in particular, a new approach for control design is presented. Section 4 describes how the mixing parameter have to be chosen. Finally, Section 5 contains the main results obtained in simulation and with a test vehicle on asphalt and snow.

2 SYSTEM MODEL

We consider a fully electric vehicle with 4WD. Each wheel is connected to an electric motor able to generate both positive and negative torques. Figure 1 plots the static characteristics of the electric motors. A low-pass filter and a time-delay complete the motor dynamics model. Furthermore, each motor has a fixed gear ratio τ.

The vehicle lateral dynamics is described by the well known linearized two degrees of freedom (DoF) single-track model in which left and right wheel are lumped together (Fig. 2). The equations are the following [22]:

$$\begin{bmatrix} \dot{\beta} \\ \dot{r} \end{bmatrix} = \begin{bmatrix} -\frac{C_f+C_r}{mv} & -1+\frac{C_r l_r - C_f l_f}{mv^2} \\ \frac{C_r l_r - C_f l_f}{I_z} & -\frac{C_f l_f^2 + C_r l_r^2}{I_z v} \end{bmatrix} \begin{bmatrix} \beta \\ r \end{bmatrix} + \\ + \begin{bmatrix} \frac{C_f}{mv} \\ \frac{C_f l_f}{I_z} \end{bmatrix} \delta + \begin{bmatrix} 0 \\ \frac{1}{I_z} \end{bmatrix} M_z \tag{1}$$

where β is the sideslip angle, r the yaw rate, $C_{f,r}$ are the front and rear cornering stiffnesses respectively, m the vehicle mass, I_z the vehicle moment of inertia, v the longitudinal velocity, $l_{f,r}$ the distance from the centre of gravity (CoG) to the front and rear axle, M_z is an external yaw moment and δ the steering angle at the ground. It is obtained from the steering wheel angle (δ_w) trough the steering wheel ratio (k): $\delta = \frac{\delta_w}{k}$. M_z is the control variable, while δ an exogenous input seen as a disturbance.

The following transfer functions are considered:

- $G_{\delta \to r}(s)$ from steering wheel at the ground to yaw rate;
- $G_{\delta \to \beta}(s)$ from steering wheel at the ground to sideslip angle;
- $G_{M_z \to r}(s)$ from yaw moment to yaw rate;
- $G_{M_z \to \beta}(s)$ from yaw moment to sideslip angle.

3 CONTROL ARCHITECTURE

The high level structure of the proposed ESC system is illustrated in Fig. 3. It is composed by three main elements:

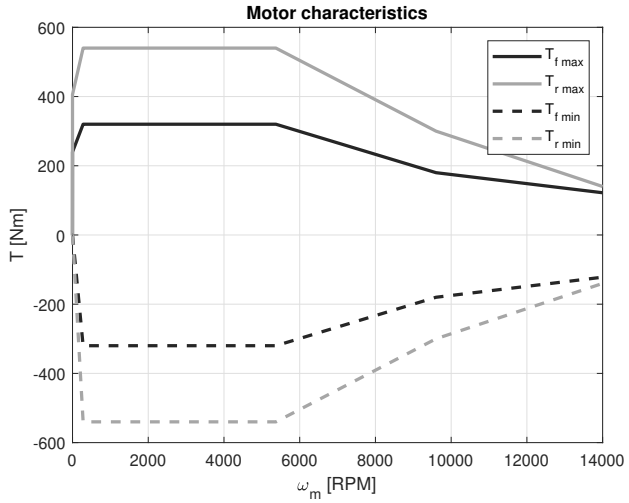

FIGURE 1: FRONT AND REAR MOTORS CHARACTERISTICS

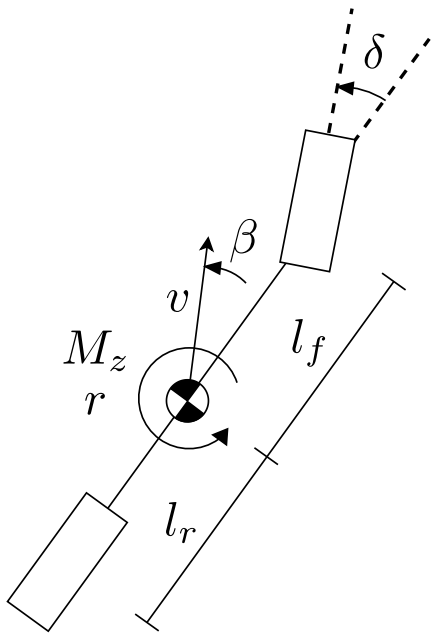

FIGURE 2: 2 DOF BICYCLE MODEL

- Reference generator;
- High level controller;
- Torque allocator.

In the next subsections, each block is described.

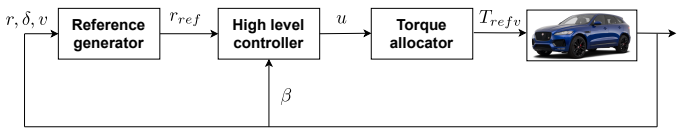

FIGURE 3: ESC SYSTEM ARCHITECTURE

3.1 Reference Generator

The reference generator has two objectives. The first one is to activate the ESC; indeed, stability control is a safety feature and has to be activated only in case of emergency. The second one is to generate a suitable reference for the control system.

Concerning the first objective, the control is enabled when e_r, *i.e.* the difference between the desired yaw rate (r_{des}) and the measured one is greater than a threshold (th_h). Conversely it is disabled when e_r is less than th_l for more than $0.5\,s$. The thresholds are chosen in simulations to guarantee an effective and less invasive as possible control intervention.

Regarding the second objective, the reference yaw rate (r_{ref}) is generated with a two steps approach. Firstly, the desired yaw rate is defined as in [1]:

$$r_{des} = \begin{cases} \frac{v}{L+v^2 K_{us}}\delta, & \text{if } \frac{v}{L+v^2 K_{us}}\delta < \frac{0.85\mu g}{v} \\ \frac{0.85\mu g}{v}, & \text{if } \frac{v}{L+v^2 K_{us}}\delta \geq \frac{0.85\mu g}{v} \end{cases} \tag{2}$$

where L is the wheelbase, g the gravitation acceleration, $K_{us} = \frac{ml_r}{C_f L} - \frac{ml_f}{C_r L}$ is the understeering coefficient of the vehicle and μ the friction coefficient. Note that r_{des} needs the knowledge of μ; but precise and fast friction estimation is difficult [23, 24]. To overcome this limitation, in the proposed ESC scheme, μ is considered fixed to 1. Thus, no friction estimation technique is required.

In the second step a logic is introduced to guarantee robustness with respect to road friction. r_{ref} is defined as:

$$r_{ref} = \begin{cases} r_{des}, & \text{if } |r| \geq |r_{des}| \wedge \text{sign}(r) = \text{sign}(r_{des}) \\ r, & \text{if } |r| < |r_{des}| \wedge \text{sign}(r) = \text{sign}(r_{des}) \\ 0, & \text{if sign}(r) \neq \text{sign}(r_{des}). \end{cases} \tag{3}$$

The first case represents the normal ESC behaviour, *i.e.* the vehicle has a higher yaw rate than the desired one thus the ESC tries to reduce r. The second one avoids undesired control action on low grip roads, indeed the desired yaw rate will be for sure higher than the vehicle one. Thus, as reference is given the vehicle yaw rate minimizing the control intervention. The third condition guarantees a sensible reference when the direction of motion is not coherent with the driver's desire. This mechanism produces a conservative control action, *i.e.* the ESC will intervene only to recover stability, whatever the road condition is. The increased robustness is paid at the cost of leaving the understeering behaviour of the vehicle unchanged. This drawback is considered acceptable by the authors since understeer is less dangerous than oversteer.

3.2 High Level Controller

The high level controller has the objective of tracking a desired reference signal by generating a yaw moment. In this paper, a strategy called *Mixed Approach* is presented. It considers both the desired yaw rate and the sideslip angle. The new output ε of the system is a convex combination of the two:

$$\varepsilon = (1-\alpha)\cdot r + \alpha \cdot (-\beta) \tag{4}$$

and thus the new reference signal is

$$\varepsilon_{ref} = (1-\alpha)\cdot r_{ref} + \alpha\cdot(-\beta_{ref}). \tag{5}$$

Usually, the scope of stability control is to avoid large β, therefore a reasonable β_{ref} will be 0. Eventually, the reference signal becomes:

$$\varepsilon_{ref} = (1-\alpha)\cdot r_{ref}. \tag{6}$$

The transfer function of the controlled system is the one between M_z and the new output ε:

$$G_{M_z\to\varepsilon} = (1-\alpha)G_{M_z\to r} - \alpha G_{M_z\to\beta}. \tag{7}$$

The initial single-input multiple-output problem has been recast in a SISO system where classical loop-shaping techniques can be used. Regarding the controller choice, a PI tuned on the obtained transfer function meets the required performance, there is no need of introducing more complex control structures, therefore:

$$M_z(s) = (\varepsilon_{ref} - \varepsilon)(k_p + \frac{k_i}{s}) \tag{8}$$

Note that if α is set to 0, the reference signal is simply r_{ref}. In this case, the high level controller will be based on the transfer function between M_z and r obtained by (1), and a pure yaw rate control is implemented. This is our benchmark control against with the *Mixed Approach* is compared. Both controllers have been tuned to guarantee a phase margin of 85 ° and a bandwidth of 3 Hz.

3.3 Torque Allocator

Since the system is over-actuated, the required M_z has to be wisely divided between the four wheels. This is the objective of the torque allocator subsystem, *i.e.* to allocate four torques to obtain the desired yaw moment. Writing a torque balance at vehicle CoG, one obtains:

$$\begin{aligned} M_{ztot} =& \cos(\delta)(F_{xfr} - F_{xfl})\frac{d_f}{2} + \sin(\delta)(F_{xfr} + F_{xfl})l_f + \\ & \cos(\delta)(F_{yfr} + F_{yfl})l_f + \sin(\delta)(F_{yfl} - F_{yfr})\frac{d_f}{2} + \\ & (F_{xrr} - F_{xrl})\frac{d_r}{2} - (F_{yrl} + F_{yrr})l_r \end{aligned} \tag{9}$$

where $d_{f,r}$ are respectively the front and rear track widths, and $F_{x,yf,r}$ are the longitudinal and lateral tyre forces. Considering that the only forces directly controllable are the longitudinal ones, the control yaw moment can be expressed as:

$$M_z = (F_{xfr} - F_{xfl})\frac{d_f}{2} + (F_{xrr} - F_{xrl})\frac{d_r}{2}, \tag{10}$$

where the hypothesis of small δ has been done. Note that, even though this may seems a strong hypothesis, the possible inaccuracies are compensated by the closed loop system. Eventually, supposing that a linear relation exists between the torque and the force: $T_w = \frac{F_x}{R_w}$, equation (10) can be written as

$$u = A\cdot T_v \tag{11}$$

where $A = \left[-\frac{d_f}{2R_w}\ \frac{d_f}{2R_w}\ -\frac{d_r}{2R_w}\ \frac{d_r}{2R_w}\right]$ and $T_v = \left[T_{fl}\ T_{fr}\ T_{rl}\ T_{rr}\right]'$.

To compute the optimum torque allocation a minimization problem is set:

$$\begin{aligned} \underset{T_i}{\text{minimize}} \quad & J(T_i) \\ \text{subject to} \quad & A\cdot T_v = M_z \\ & T_i \le hb_i \\ & T_i \ge lb_i \end{aligned} \tag{12}$$

where hb_i and lb_i are respectively the highest and lowest motor torque for each corner. The cost function $J(T_i) = T_{fl}^2 + T_{fr}^2 + T_{rl}^2 + T_{rr}^2$ aims at minimizing the torques at each wheel. Note that this makes the hypothesis of the relation between torque and force less critical.

Many techniques to solve online the control allocation problem can be found in the literature (see *e.g.* [25–28]), the advantages of online approaches are that actuators failures and time varying saturations can be considered. For the sake of simplicity, since control allocation is not the focus of this paper, the optimization problem (12) is solved offline obtaining the look-up tables represented in Fig. 4. It can be highlighted how the control allocation uses all available actuators: 2 exerting positive torque and 2 negative one.

4 α choice

Deciding α is not trivial and straightforward, as stated in [20], weighting yaw rate and sideslip is a challenging problem in terms of linear control system. First of all recall that the two extrema, *i.e.* $\alpha = 0$ and $\alpha = 1$, represent either a r or a β based controller. The first one is what we have called *pure yaw rate control* and is used as benchmark. Intuitively, the second one, considering $\beta_{ref} = 0$, forces the vehicle to go straight. This is not the objective of an ESC and is not suitable a priori.

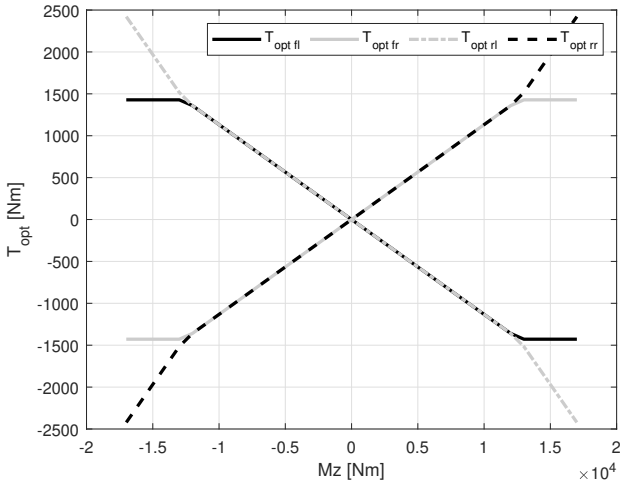

FIGURE 4: OPTIMUM TORQUE ALLOCATION

To analyse the effect of weighting β, the steady-state yaw rate and sideslip obtained for a steering step for different $\alpha \in [0,1]$ are computed. Take in account the complete control scheme represented in Fig. 5. Note that r_{ref}, neglecting the saturation, coincides with $G_{\delta \to r}(0)$ and suppose that the requested yaw moment is precisely obtained by the torque allocator. Furthermore, for the sake of analysis, consider $C(s) = k$. Figure 6 shows the normalized value of r and β with respect to the benchmark controller ($\alpha = 0$). As can be seen, the higher α the lower values of both r and β. Thus choosing $\alpha \neq 0$ will reduce the sideslip angle but as side effect will also change the obtained yaw rate, meaning that the driver will feel a different response ($\alpha = 0$ coincides with the ideal behaviour). On the other hand, since the trend is non linear and β is reduced more and r, a small α will still guarantee a sensible response attenuating β.

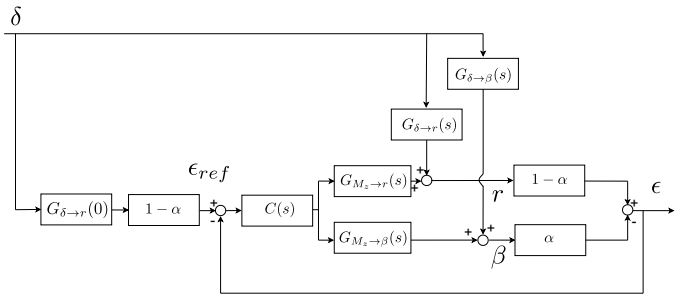

FIGURE 5: MIXED APPROACH COMPLETE BLOCK DIAGRAM

Now consider a different scenario in which μ changes and compare two cases:

A. the reference generator has perfect knowledge of the friction coefficient and α is set to 0 (ideal yaw rate control);
B. the reference generator has a fixed $\mu = 1$ and α varies.

To understand the advantage of weighting β, $\gamma = \frac{r_B(\mu=1,\alpha)}{r_A(\mu,\alpha=0)}$, *i.e.* the yaw rate of case B divided by the one of case A for different α and μ, will be analysed. The ideal result would be $\gamma = 1$, but since the reference generator of case B has a fixed friction coefficient it will force the vehicle to steer more ($\gamma > 1$) on low grip surfaces. By increasing α, the weight of yaw rate reference in ϵ_{ref} diminishes. Therefore, the control is less sensitive to reference generator uncertainties. In particular, Fig. 7 resumes these results. In case of very low friction, a wrong reference, with $\alpha = 0$, will force the vehicle to rotate about three times faster. On the other hand, as previously highlighted, α too high will strongly attenuate the yaw rate. This second analysis will suggest a medium-high α to reduce the sensitivity with respect to road conditions.

Eventually, merging the two qualitative analyses, $\alpha = 0.5$ is chosen to guarantee a sensible yaw rate response, β attenuation and road condition robustness. These results have been obtained with a constant longitudinal speed equal to 80 km/h, anyway by changing the velocity the conclusions are the same.

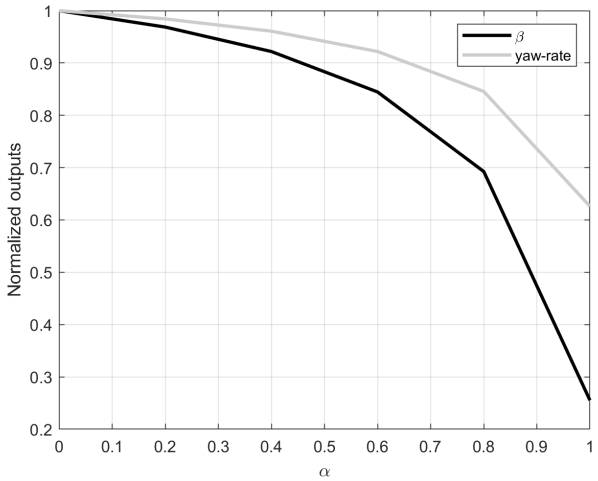

FIGURE 6: NORMALIZED YAW RATE AND SIDESLIP FOR DIFFERENT α

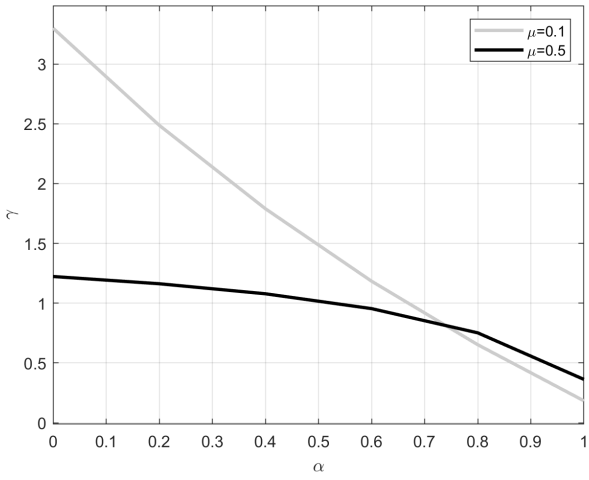

FIGURE 7: RATIO BETWEEN THE STEADY-STATE YAW RATE OF CASE B (WRONG AND FIXED μ, α VARYING) AND THE ONE OF CASE A (EXACT μ KNOWLEDGE, $\alpha = 0$) FOR DIFFERENT α AND μ

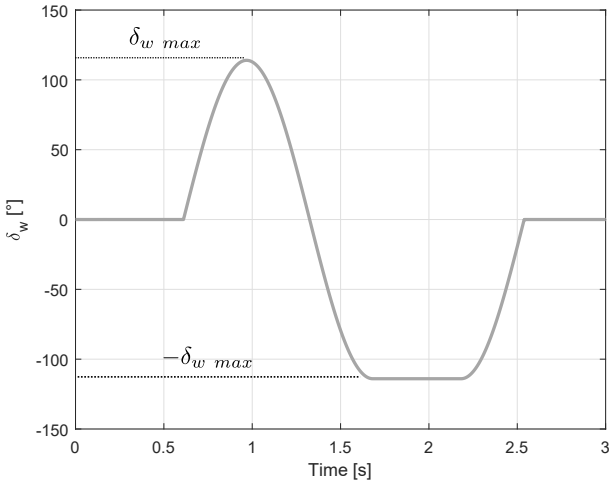

FIGURE 8: EXAMPLE OF A SWD STEERING INPUT

5 RESULTS

5.1 Manoeuvre

ESC certification procedure is regulated by EU law [29]. It consists in a series of sine with dwell (SWD) (Fig. 8) at 80 km/h with increasing amplitude. Once all the tests have been done, yaw rate and lateral position are post-processed to validate the manoeuvre.

Note that the ESC procedure specifies a high friction road. In this work, high friction ($\mu \in (0.7,\ 1]$)), medium friction ($\mu \in (0.4,\ 0.7]$)) and low friction ($\mu \in [0.1,\ 0.4]$) roads are considered.

5.2 Simulation Results

The proposed control scheme has been tested in simulation following the ESC procedure previously described. First of all the validity of the solution has been proved using the *pure yaw rate approach* ($\alpha = 0$), then it has been compared with the *Mixed Approach* ($\alpha = 0.5$). Both the controllers have been tuned to have similar performance in closed loop. Concerning the simulation environment, Matlab and CarMaker (a multi body simulation software) [30] have been utilized. In CarMaker a vehicle has been created to resemble the real one, the main parameters are listed in Table 1.

Figure 9 depicts examples of the reference generated by (3) for different grips without the ESC. In particular, Fig. 9a shows a high $\delta_{w\ max}$ and μ in which the desired yaw rate is lower than the measured one both in the first and in the second phase. Thus r_{ref} will be equal to r_{des} most of the time to recover vehicle stability. On the other hand, Fig. 9b highlights how r_{ref} is equal to r when

TABLE 1: VEHICLE PARAMETERS

Parameter	Symbol	Value
Mass	m	2648 kg
Moment of inertia	I_z	4591 kgm^2
Distance of the CoG from front axle	l_f	1.517 m
Distance of the CoG from rear axle	l_r	1.352 m
Front track width	d_f	1.656 m
Rear track width	d_r	1.656 m
Front cornering stiffness	C_f	165000 N/rad
Rear cornering stiffness	C_r	240000 N/rad
Steering wheel ratio	k	14.6

we are on low grip surfaces avoiding that an unfeasible reference is tracked. In any case, if the driver reduces or modifies the direction of the steering action the reference generation mechanism is such that stability will be guaranteed.

Both controllers pass the nominal certification test, reducing μ to medium and low the systems continue to have satisfactory performance, just one SWD is not passed with the pure yaw rate approach: $\delta_{w\ max} = 38\ °$, $\mu = 0.1$.

Figure 10 compares the mixed control scheme with the benchmark for the most aggressive manoeuvre. In the bottom plot the yaw rates are represented; it can be observed how the two do not differ since sideslip contribution is negligible. The centre plot, where sideslips are shown, illustrates how β is reduced

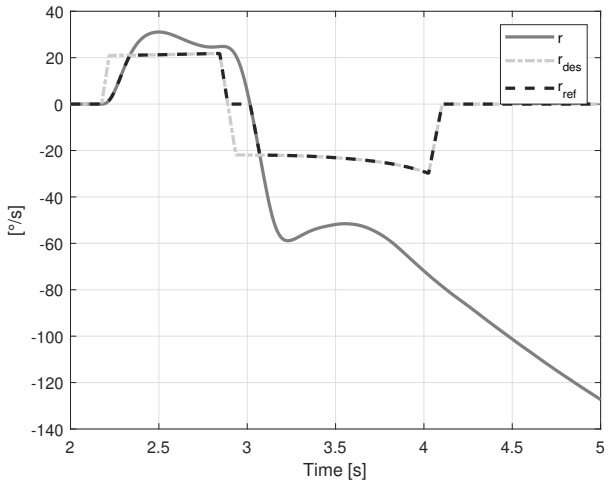

(a) $\delta_{w\ max} = 270\,[^\circ], \mu = 1$

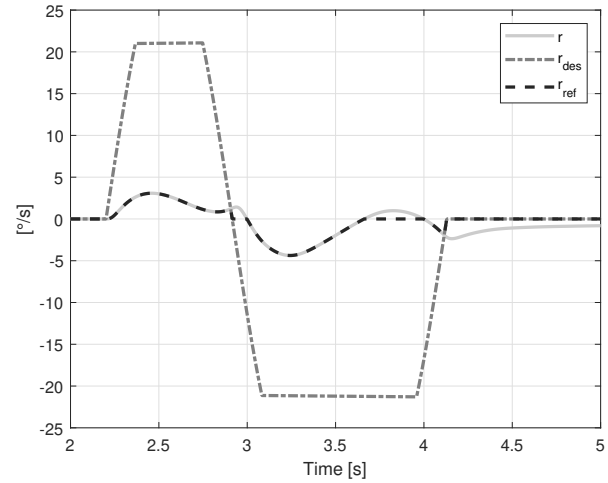

(b) $\delta_{w\ max} = 76\,[^\circ], \mu = 0.1$

FIGURE 9: EXAMPLES OF DESIRED AND REFERENCE YAW RATE DURING AN OPEN-LOOP SWD FOR DIFFERENT μ AND $\delta_{W\ MAX}$

more than the yaw rate. Lastly, it can be noticed that vehicle stability is maintained in both the cases and SWD requirements are satisfied. Indeed, the open-loop case, shown in Fig. 9a, results in the vehicle drifting.

Figure 11 shows the results obtained for $\mu = 0.1$ and $\delta_{w\ max} = 38$ ° in which the sideslip is hugely reduced with the *Mixed Approach*. Furthermore, it can be noticed how the pure yaw rate strategy is able to recover the vehicle stability in terms of yaw rate but when it is deactivated (at about 5.2 *s*) the car starts to rotate again. It is clear, by looking at the sideslip, that controlling just one variable is not enough at low grip, indeed β diverges. On the other hand, the *Mixed Approach* keeps β limited and helps the vehicle to maintain the stability.

Eventually, the *Mixed Approach* is compared with the approach proposed by Lenzo et al. in [20]. They diminish the reference yaw rate according to the sideslip amplitude. We used the safest configuration proposed by the authors, and since their scheme based is on yaw rate we used our controller tuned with $\alpha = 0$. No additional logic is present in the work and therefore we did not applied our proposed logic to their reference. Figure 12 shows the comparison in a SWD test on low grip. It is evident that diminishing the reference is not enough to keep the sideslip limited. Furthermore, once the vehicle start drifting is impossible to recover stability. The *Mixed Approach*, by directly weighting β, reduces the sideslip in any case.

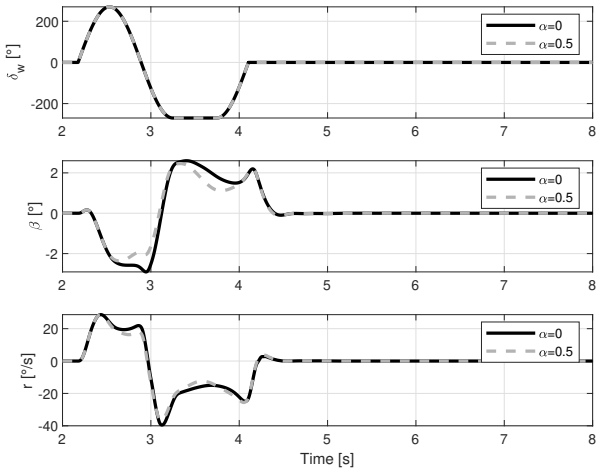

FIGURE 10: COMPARISON BETWEEN YAW RATE ($\alpha = 0$) AND MIXED ($\alpha = 0.5$) CONTROLLERS. SWD WITH $\delta_{W\ MAX} = 270\,[^\circ]$ AND $\mu = 1$

5.3 Experimental Results

The proposed ESC has been experimentally validated on a full electric SUV with 4 electric motors at two proving grounds to test the vehicle on different road conditions (the second test site was a winter proving ground). We implemented the control scheme using dSpace and MicroAutoBox with a sampling period of 0.01 s. Regarding the quantities that are usually not measurable, *i.e.* β and v, an algorithm present in the literature has been chosen and implemented to estimate the values (for the sake of space details about the algorithm are not reported, for further information regarding the method see [21]).

On dry asphalt, due to safety constraints and track limitations, the most aggressive tests have been done with $\delta_{w\ max}$ about

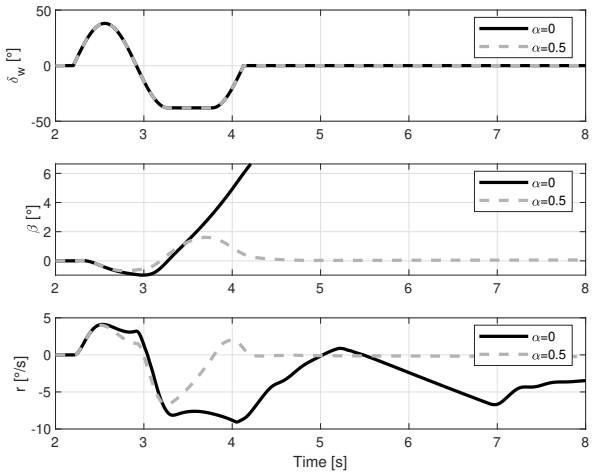

FIGURE 11: COMPARISON BETWEEN YAW RATE ($\alpha = 0$) AND MIXED ($\alpha = 0.5$) CONTROLLERS. SWD WITH $\delta_{W\ MAX} = 38\,[^\circ]$ AND $\mu = 0.1$

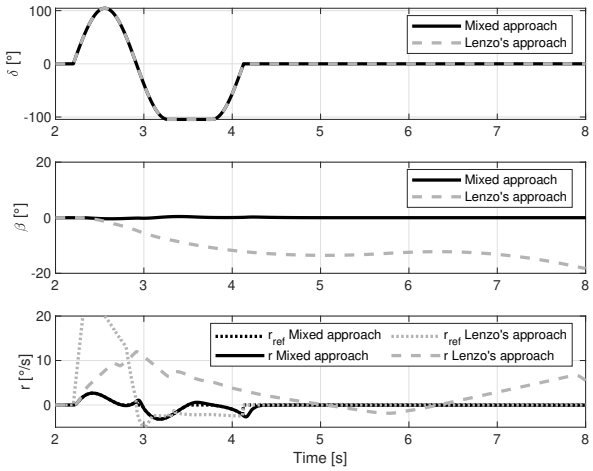

FIGURE 12: COMPARISON BETWEEN MIXED ($\alpha = 0.5$) AND LENZO'S APPROACH. SWD WITH $\delta_{W\ MAX} = 104\,[^\circ]$ AND $\mu = 0.1$

100° and $v = 60$ km/h, anyway, it is enough to bring the vehicle to instability. Fig. 13 shows the comparison between open and closed loop with the pure yaw rate approach, moreover Fig. 14 shows the comparison between the two presented strategies. As expected, both ESCs keep the vehicle stable. Furthermore, since sideslip is not critical on high grip the mixed approach does not modify the yaw rate.

The controllers have been also tested on snow with a SWD at 50 km/h. Fig. 15 shows a comparison between the open and closed loop case in which the effectiveness of the pure yaw rate approach can be appreciated even though high β is reached. On the other hand, Fig. 16 demonstrates that the *Mixed Approach* significantly reduces the sideslip angle; indeed, the peak value is halved.

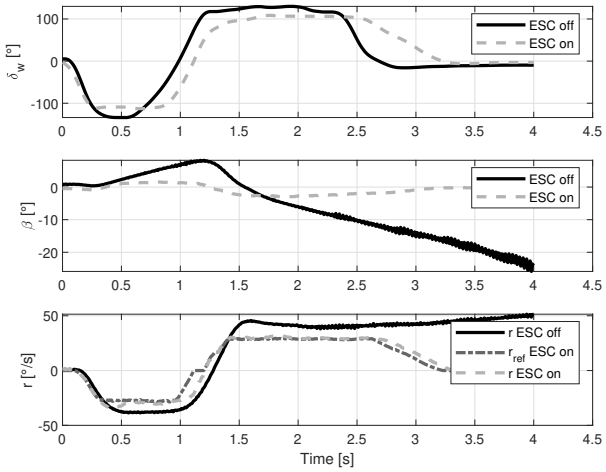

FIGURE 13: SWD WITH ESC OFF AND ON (PURE YAW RATE APPROACH) ON ASPHALT - EXPERIMENTAL RESULTS.

6 CONCLUSION

In this paper, we presented a mixed yaw rate and sideslip approach. To the best of author's knowledge, there is only one contribution that modifies the reference signal. The proposed solution do not explicitly constrains the sideslip. Furthermore, the *Mixed Approach* permits to design the regulator with SISO techniques. Based on a mix of yaw rate and sideslip angle, the controller is able to reduce β while keeping r as similar as possible to the *natural* behaviour. Introducing β in the loop ensures more robustness on low friction scenarios. We motivated the rationale to choose α: crucial parameter for the mixed control. Low α will guarantee a response of the system similar to the one expected by the driver. On the other hand, the more β is weighted in the loop the less the vehicle will suffer from friction change; $\alpha = 0.5$ is then chosen.

Finally, the *Mixed Approach* is part of a comprehensive structure for ESC, including an effective way to generate the reference and an optimum offline allocation of the control action. The reference generator is robust with respect to the friction coefficient.

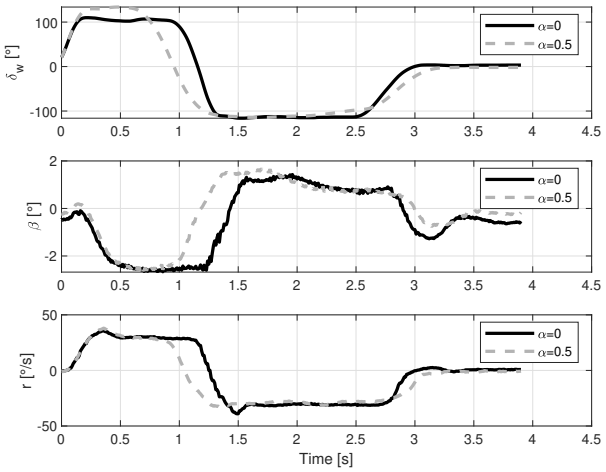

FIGURE 14: COMPARISON BETWEEN YAW RATE ($\alpha = 0$) AND MIXED ($\alpha = 0.5$) CONTROLLERS. SWD ON THE TEST VEHICLE ON ASPHALT - EXPERIMENTAL RESULTS

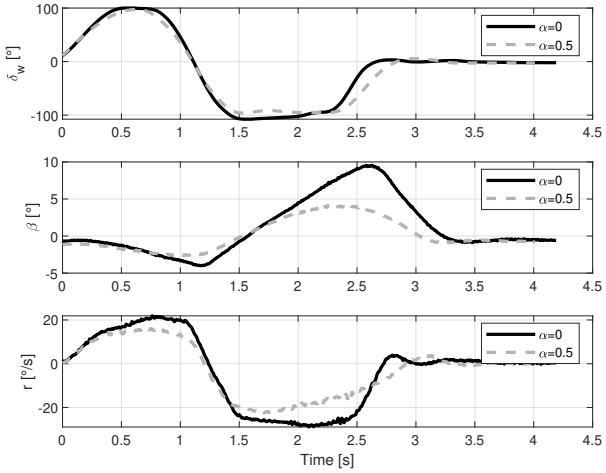

FIGURE 16: COMPARISON BETWEEN YAW RATE ($\alpha = 0$) AND MIXED ($\alpha = 0.5$) CONTROLLERS. SWD ON THE TEST VEHICLE ON SNOW - EXPERIMENTAL RESULTS

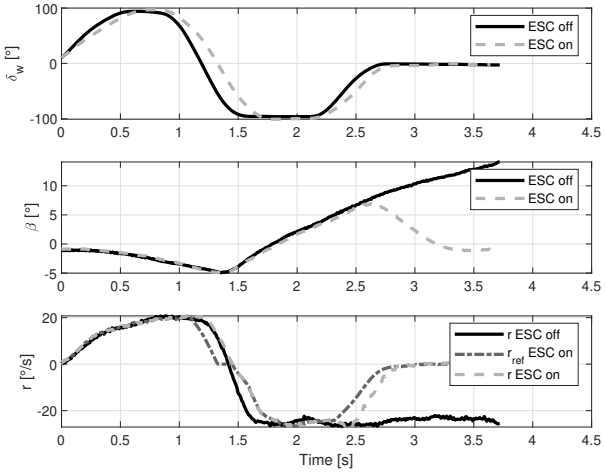

FIGURE 15: SWD WITH ESC OFF AND ON (PURE YAW RATE APPROACH) ON SNOW - EXPERIMENTAL RESULTS.

Eventually, the proposed controllers have been validated in simulation and with a test vehicle. The ESC system proved its effectiveness both on asphalt and snow.

References

[1] Rajamani, R., 2011. *Vehicle Dynamics and Control*. Mechanical Engineering Series. Springer US.

[2] Liebemann, E. K., Meder, K., Schuh, J., and Nenninger, G., 2004. "Safety and performance enhancement: The bosch electronic stability control (esp)". Convergence Transportation Electronics Association.

[3] van Zanten, A. T., 2000. "Bosch esp systems: 5 years of experience". SAE International.

[4] Rosenberger, M., Uhlig, R. A., Koch, T., and Lienkamp, M., 2012. Combining regenerative braking and anti-lock braking for enhanced braking performance and efficiency. Tech. rep., SAE Technical Paper.

[5] Hori, Y., 2002. "Future vehicle driven by electricity and control-research on four wheel motored" uot electric march ii"". In 7th International Workshop on Advanced Motion Control. Proceedings (Cat. No. 02TH8623), IEEE, pp. 1–14.

[6] Manning, W., and Crolla, D., 2007. "A review of yaw rate and sideslip controllers for passenger vehicles". *Transactions of the Institute of Measurement and Control,* ***29***(2), pp. 117–135.

[7] Hu, J., Wang, Y., Fujimoto, H., and Hori, Y., 2017. "Robust yaw stability control for in-wheel motor electric vehicles". *IEEE/ASME Transactions on Mechatronics,* ***22***(3), pp. 1360–1370.

[8] De Novellis, L., Sorniotti, A., Gruber, P., and Pennycott, A., 2014. "Comparison of feedback control techniques for torque-vectoring control of fully electric vehicles". *IEEE Transactions on Vehicular Technology,* ***63***(8), Oct, pp. 3612–3623.

[9] Canale, M., Fagiano, L., Ferrara, A., and Vecchio, C., 2008. "Vehicle yaw control via second-order sliding-mode

technique". *IEEE Transactions on Industrial Electronics,* ***55***(11), pp. 3908–3916.

[10] Goggia, T., Sorniotti, A., De Novellis, L., Ferrara, A., Gruber, P., Theunissen, J., Steenbeke, D., Knauder, B., and Zehetner, J., 2014. "Integral sliding mode for the torque-vectoring control of fully electric vehicles: Theoretical design and experimental assessment". *IEEE Transactions on Vehicular Technology,* ***64***(5), pp. 1701–1715.

[11] Chen, B. C., and Kuo, C. C., 2014. "Electronic stability control for electric vehicle with four in-wheel motors". *International Journal of Automotive Technology,* ***15***, 06, pp. 573–580.

[12] Shibahata, Y., Shimada, K., and Tomari, T., 1993. "Improvement of vehicle maneuverability by direct yaw moment control". *Vehicle System Dynamics,* ***22***(5-6), pp. 465–481.

[13] Chung, T., and Yi, K., 2006. "Design and evaluation of side slip angle-based vehicle stability control scheme on a virtual test track". *IEEE Transactions on control systems technology,* ***14***(2), pp. 224–234.

[14] Tchamna, R., and Youn, I., 2013. "Yaw rate and side-slip control considering vehicle longitudinal dynamics". *International Journal of Automotive Technology,* ***14***(1), pp. 53–60.

[15] Ding, S., Liu, L., and Zheng, W. X., 2017. "Sliding mode direct yaw-moment control design for in-wheel electric vehicles". *IEEE Transactions on Industrial Electronics,* ***64***(8), pp. 6752–6762.

[16] Geng, C., Mostefai, L., Denaï, M., and Hori, Y., 2009. "Direct yaw-moment control of an in-wheel-motored electric vehicle based on body slip angle fuzzy observer". *IEEE Transactions on Industrial Electronics,* ***56***(5), pp. 1411–1419.

[17] Esmailzadeh, E., Goodarzi, A., and Vossoughi, G., 2003. "Optimal yaw moment control law for improved vehicle handling". *Mechatronics,* ***13***(7), pp. 659–675.

[18] Kaiser, G., 2015. *Torque Vectoring-Linear Parameter-Varying Control for an Electric Vehicle*. Technische Universität Hamburg.

[19] Liberzon, D., and Morse, A. S., 1999. "Basic problems in stability and design of switched systems". *IEEE Control Systems Magazine,* ***19***(5), pp. 59–70.

[20] Lenzo, B., Zanchetta, M., Sorniotti, A., Gruber, P., and De Nijs, W., 2020. "Yaw rate and sideslip angle control through single input single output direct yaw moment control". *IEEE Transactions on Control Systems Technology*, pp. 1–16.

[21] Galluppi, O., Corno, M., and Savaresi, S. M., 2018. "Mixed-kinematic body sideslip angle estimator for high performance cars". In 2018 European Control Conference (ECC), IEEE, pp. 941–946.

[22] Abe, M., 2015. *Vehicle handling dynamics: theory and application*. Butterworth-Heinemann.

[23] Ahn, C., Peng, H., and Tseng, H. E., 2011. "Robust estimation of road frictional coefficient". *IEEE Transactions on Control Systems Technology,* ***21***(1), pp. 1–13.

[24] Muller, S., Uchanski, M., and Hedrick, K., 2003. "Estimation of the maximum tire-road friction coefficient". *J. Dyn. Sys., Meas., Control,* ***125***(4), pp. 607–617.

[25] Schofield, B., 2008. "On active set algorithms for solving bound-constrained least squares control allocation problems". In 2008 American Control Conference, pp. 2597–2602.

[26] Harkegard, O., 2002. "Efficient active set algorithms for solving constrained least squares problems in aircraft control allocation". In Proceedings of the 41st IEEE Conference on Decision and Control, 2002., Vol. 2, pp. 1295–1300 vol.2.

[27] Bodson, M., 2002. "Evaluation of optimization methods for control allocation". *Journal of Guidance, Control, and Dynamics,* ***25***(4), pp. 703–711.

[28] Oppenheimer, M. W., Doman, D. B., and Bolender, M. A., 2006. "Control allocation for over-actuated systems". In 2006 14th Mediterranean Conference on Control and Automation, pp. 1–6.

[29] Regulation no 140 of the economic commission for europe of the united nations (un/ece) — uniform provisions concerning the approval of passenger cars with regard to electronic stability control (esc) systems [2018/1592].

[30] CarMaker | IPG automotive. Accessed: 2019-03-14.